scientific reports

Check for updates

OPEN

UCMSC-derived exosomes ameliorate dry eye disease pathogenesis by modulating neutrophils on Th17/Treg balance

Yuxing Gong[1,2,10], Yufei Ding[3,4,10], Jingyi Yang[1,4], Tao Ding[1,2], Bin Li[1,2], Junfeng Ma[5], Wahid Shah[2,6], Youcai Deng[7], Ping Duan[8,9], Yu Zhang[1]✉ & Yuan Gao[2,6]✉

Dry eye disease (DED) is a chronic ocular surface disorder characterized by Th17/Treg cells imbalance, particularly prevalent among elderly females. Current treatment approaches are evolving from merely providing symptomatic relief to targeting immune dysfunction. Mesenchymal stem cell-derived exosomes (MSC-Exos) have demonstrated the ability to modulate the immune response and promote corneal epithelial cell regeneration in DED. Nonetheless, the precise mechanism through which MSC-Exos exert these effects is not yet fully understood. Consequently, the objective of this study was to explore the mechanisms behind the therapeutic effects of umbilical cord mesenchymal stem cell-derived exosomes (UCMSC-Exos) in a murine model of DED. We discovered that UCMSC-Exos stimulated human corneal epithelial cell lines wound healing in vitro. The topical or systemic administration of UCMSC-Exos significantly altered cytokine expression by neutrophils, leading to a reduction in proinflammatory cytokine expression and an increase in anti-inflammatory cytokine expression. This shift in the cytokine profile reestablished the Treg/Th17 cells balance, resulting in decreased inflammation and alleviation of DED symptoms, with younger mice showing more pronounced benefits. These results highlight the potential of UCMSC-Exos as a therapeutic approach for DED that modulates immune dysregulation and enhances ocular surface repair.

Keywords Dry eye disease, Exosomes, Umbilical cord mesenchymal stem cells, Neutrophils, Th17/Treg cells balance

Dry eye disease (DED) is a chronic immune disorder with an estimated global prevalence ranging from 5 to 50% [1,2]. Female gender, older age, connective tissue disease, and some medications[3], as well as extended use of electronic devices, poor ocular hygiene, and prolonged contact lens usage[4], are risk factors for DED. DED is characterized by an imbalance in ocular surface immune homeostasis[5–7], including altered proportions of immune cells, such as dendritic cells[8,9], macrophages[10], and T cells (including Th1, Th17, and Treg cells)[11–13]. Dysregulated expression of inflammatory cytokines (IFN-γ, TNFα, IL-1β, IL-6, IL-20, and TGFβ) by these immune cells has also been observed[14,15]. The resulting inflammation leads to a reduction in the stability of the tear film and injury to the ocular surface[16,17]. A typical pharmacological strategy for the treatment of DED is the prolonged use of artificial tears; however, this approach does not address the underlying immune dysregulation. Other treatments include topical corticosteroids, nonsteroidal anti-inflammatory drugs (NSAIDs), and

[1] Key Laboratory of Cellular Physiology (Shanxi Medical University), Ministry of Education, and the Department of Physiology, Shanxi Medical University, Taiyuan 030001, Shanxi, China. [2]Translational Medicine Research Center, Shanxi Medical University, Taiyuan 030001, China. [3]Shanxi Provincial Key Laboratory of Drug Synthesis and Novel Pharmaceutical Preparation Technology, School of Pharmacy, Shanxi Medical University, Taiyuan 030001, Shanxi, China. [4]Academy of Medical Sciences, Shanxi Medical University, Jinzhong 030006, Shanxi, China. [5] Chongqing Key Lab of Ophthalmology, Chongqing Eye Institute, Chongqing Branch of National Clinical Research Center for Ocular Diseases, The First Affiliated Hospital of Chongqing Medical University, Chongqing 400038, China. [6]Shanxi Eye Hospital Affiliated to Shanxi Medical University, Taiyuan 030002, China. [7]Department of Pharmacology, College of Pharmacy, Army Medical University, Chongqing 400038, China. [8]Southwest Hospital/Southwest Eye Hospital, Army Medical University, Chongqing 400038, China. [9]Key Lab of Visual Damage and Regeneration & Restoration of Chongqing, Chongqing 400038, China. [10]Yuxing Gong and Yufei Ding contributed equally to this work. ✉email: zhyucnm@163.com; gaoyuan8785@126.com

immunosuppressants[18–21], but many of these medications contain preservatives that can exacerbate DED symptoms and signs, and prolonged use of corticosteroids and immunosuppressants can cause adverse reactions such as osteoporosis and infection[22]. Furthermore, a few reports have highlighted an association between topical NSAID use and corneal complications such as corneal ulceration, melt, and perforation[23], making this a suboptimal treatment option. Importantly, no current therapeutic approach for DED directly addresses immune cell imbalance and altered cytokine expression levels.

Recently, stem cell-based therapies have been investigated for DED[24]. However, the use of stem cell–based approaches is hampered by ethical concerns and the risks of administering whole cells as a therapy[25,26]. Exosomes are extracellular vesicles secreted by cells that can encapsulate various components of their cells of origin, such as DNA, RNA, proteins, lipids, and metabolites[27]. They are regarded as a superior treatment option to stem cells themselves, as they are less likely to provoke an immune response than administration of intact cells. Exosomes, with a size range of 40–160 nm, can effectively penetrate the corneal epithelial barrier following topical administration, enabling targeted delivery of therapeutic cargo to the corneal stroma and subepithelial layers[28]. A previous study demonstrated that mesenchymal stem cell-derived exosomes (MSC-Exos) effectively treat DED[29] by modulating the immune response and facilitating corneal epithelial cell regeneration. Moreover, MSC-Exos alleviate DED associated with graft-versus-host disease by reprogramming macrophages from a proinflammatory M1 phenotype towards an immunosuppressive M2 phenotype via miR-204-mediated targeting of the IL-6/IL-6R/Stat3 pathway[30]. However, the detailed mechanism underlying these effects is still unclear.

Thus, the aim of this study was to investigate the mechanism by which umbilical cord mesenchymal stem cell-derived exosomes (UCMSC-Exos) exert therapeutic effects in the context of DED. We employed both a murine model and human epithelial cell lines and found that UCMSC-Exos altered neutrophil infiltration into the eye and modified their cytokine expression profile, resulting in increased anti-inflammatory cytokine secretion and decreased pro-inflammatory cytokine secretion. This led to restoration of the Th17/Treg balance, which reduced ocular inflammation and alleviated dry eye pathogenesis. Importantly, this modulation of the neutrophil-T cell axis was more effective in younger female mice than in older female mice. Our findings provide a theoretical framework for DED treatment and highlight UCMSC-Exos as a potential therapeutic agent for this condition.

Materials and methods

Cell lines and culture conditions

Human umbilical cord mesenchymal stem cells (UCMSCs) (approval number: 2023SJL66) were grown in DMEM/F12 (Gibco) supplemented with 10% FBS (Gibco), 100 U/mL penicillin (Invitrogen), and 100 µg/mL streptomycin (Invitrogen) at 37 °C with 5% CO_2, and the medium was refreshed every three days, as described previously[31]. Cells from passages three to six were used in the experiments. Human corneal epithelial cells (HCECs) were purchased from Pricella (CP-H128) and cultured in HCEC medium (CM-H128) at 37 °C with 5% CO_2.

Isolation and analysis of UCMSC-Exos

UCMSC supernatant was collected and centrifuged at 300 *g* for 10 min at 4 °C to eliminate intact cells, followed by centrifugation at 2000 × g for 20 min at 4 °C. The resulting supernatant was then centrifuged at 10,000 × g for 30 min at 4 °C to remove microvesicles (larger than exosomes) and passed through a 0.22-µm filter (Millex, SLGPR33RB) to remove cell debris. Next, the filtrate was centrifuged twice at 100,000 *g* for 70 min at 4 °C (Type 70Ti rotor, Beckman Coulter) to isolate the UCMSC-Exos.

To perform morphological analysis of the isolated exosomes, the exosomes were diluted to 0.1 µg/µL (20 µL) and dropped onto Formvar/carbon-coated electron microscopy grids within 5 min. Uranium hydrogen oxide acetate (2%, pH = 7.0) (20 µL) was then dropped on the copper net for 1 min, followed by drying the copper mesh under an incandescent lamp for 20 min. Exosome morphology was then observed using a transmission electron microscope (Japan Electron 1011).

The size of the isolated exosomes was determined using a Zetasizer Nano ZSE (Malvern Panalytical), and the results were analyzed using Zetasizer Software 8.01.4906. Nanosight readings were performed using exosomes diluted in PBS that had been previously depleted of nanoparticles by ultracentrifugation for increased accuracy. The Nanosight measurement setup is distinct from the Zetasizer Nano ZSE, which focuses on directly visualizing and analyzing exosomes in diluted samples.

In vitro wound healing assay

HCECs were cultured in a 6-well plate until they reached 90% confluency. A straight scratch was made by dragging a 200 µL sterile pipette tip across the monolayer surface to create a wound of about 1 mm in width. The monolayer was gently washed to remove detached cells, and fresh culture medium was added. Next, UCMSC-Exos (2.5×10^{10} particles/mL) were added to the culture medium and incubated for 48 h. Images of the scratch wound were taken using an inverted microscope system (Leica) and the width of the scratch was measured using Image J software to assess wound closure. For each time point, five random fields of view were selected from each well, and a total of 15 images were taken for each experimental condition.

Experimental animals

Fifteen-week-old and fifty-week-old C57BL/6 female mice were purchased from Cyagen (Suzhou, China) and housed in a specific pathogen-free (SPF) facility at room temperature with a 12/12-hour light/dark cycle and *ad libitum* access to food and water at the Animal Care Center of Shanxi Medical University. Only female mice were used due to the predominance of DED in female patients, and two different ages were used to assess age-related differences in DED symptoms. All animal experiments were approved by the Animal Care Committee of Shanxi

Medical University (approval number: 2023 -133) and conducted according to the institution's laboratory animal welfare guidelines. All animal experiments were conducted in accordance with the ARRIVE guidelines.

Experimental dry eye model

Female C57BL/6 mice (15-week-old and 50-week-old) were placed in individually vented cages with a fan producing continuous airflow with low humidity (20–30%) and treated with 0.1 mL of a 10 mg/mL scopolamine hydrobromide (Sigma-Aldrich, St Louis, MO) solution formulated in sterile saline via subcutaneous injection for five consecutive days, followed by a reduced dose (0.1 mL of a 5 mg/mL solution) for 10 days, to inhibit lacrimal gland function. Injections were delivered three times per day (9 AM, 2 PM, and 7 PM) into alternating hindquarters. On day 15, all mice were euthanized with sodium pentobarbital, placed on ice, and subjected to cardiac perfusion. Then, whole eyes, corneas, and eye-draining lymph nodes were harvested for further experiments, as described previously (Fig. 1A)[32,33].

Fluorescein staining

To assess damage to the ocular surface, the conjunctival sacs of intact mouse eyes were instilled with 5 µL of 0.5% fluorescein sodium solution (Sigma, F6377) and incubated at room temperature for 30 s. The ocular surface was then examined under a microscope (Leica) equipped with a cobalt blue filter. Corneal epithelial damage was assessed by dividing the cornea into five regions and grading each on a scale from 0 to 4, where 0 indicates no damage, 1 represents mild punctate staining, 2 indicates moderate punctate staining, 3 denotes severe punctate staining with partial confluence, and 4 signifies severe damage with complete confluence of staining.

Schirmer's test

A 5-mm cotton thread was carefully placed in the lateral canthus of the mouse's eye, ensuring contact with the conjunctival sac. The thread was held in place for 30 s to allow absorption of tear fluid. After 30 s, the thread was removed, and the length of the moistened portion (red coloration due to phenol red) was measured in millimeters. The length of the moistened area (in millimeters) corresponds to the volume of tear production.

Immunohistochemistry

For immunofluorescence imaging, corneas with complete limbi and retinas were fixed with 4% formaldehyde (Solarbio, P1110), permeabilized with 0.25% Triton X-100 (Solarbio, T8200) and blocked with 3% bovine serum albumin (BSA, Sigma-Aldrich). Next, the corneas were stained with FITC anti-mouse Ly-6G antibody (Biolegend, 127606) for neutrophils and Alexa Fluor 647® anti-mouse CD31 Antibody (Biolegend, 102416) for limbal vessel endothelium. The cornea was then counter-stained with 4′, 6-diamidino-2-phenylindole (Solarbio, C0065) to assess nuclear morphology. Each step was followed by three washes with PBS. Radial cuts were made in the cornea so that they could be flattened under a coverslip, and they were then mounted with anti-fading mounting medium (Solarbio, S2100). The flat-mounted corneas were observed using a confocal microscope (Leica, SP8) with a 40 × lens so that the full diameter of the cornea (from limbus to limbus) was visible within a single field of view. The total number of positively stained cells throughout the depth of the cornea from the epithelial surface to the endothelial surface was counted.

Flow cytometry

Eye-draining lymph nodes and corneal tissues were ground and filtered through a 70-µm strainer (BD Biosciences, San Diego, CA, USA) to generate a single-cell suspension. The resulting cells were washed with 2% FBS and then incubated with the following antibodies, protected from light, for 30 min at 4 °C: APC/Cyanine7 anti-mouse CD3e (Biolegend, 100330), FITC anti-mouse CD4 (Biolegend, 100406), brilliant violet 421™ anti-mouse CD196 (CCR6) (Biolegend, 129818), PE anti-mouse CD25 (Biolegend, 102008), Alexa Fluor® 700 anti-mouse CD45 (Biolegend, 103128), APC/Cyanine7 anti-mouse/human CD11b (Biolegend, 101226), FITC anti-mouse Ly-6G (Biolegend, 127606), and PE anti-human ki67 (Biolegend, 151210). Flow cytometry was performed on BD LSR Fortessa Cell Analyzer (BD, 647800), and FlowJo software v10.8.1 (https://www.flowjo.com/flowjo/download) was used for data analysis.

Western blotting

Proteins were extracted from UCMSC-Exos, and the total protein concentration was determined by BCA assay (Beyotime, P0010). Equal amounts of protein (25 µL per sample) were loaded onto 10% SDS-PAGE gels (Bio-Rad), subjected to electrophoresis, and electro-transferred onto PVDF membranes (Millipore, IPVH00010). The membranes were blocked with 5% (w/v) non-fat dry milk at 4 °C for 2 h followed by overnight incubation with the following primary antibodies: anti-TSG101 (Cell Signaling Technology, 72312 S, 1:500), anti-ANXA1 (Abcam, ab214486, 1:500), anti-CD9 (Cell Signaling Technology, 13174 S, 1:500), and anti-CD81 (Cell Signaling Technology, 56039 S, 1:500), anti-CD63 (Cell Signaling Technology, 52090 S, 1:500), anti-CANX (Abcam, ab22595). Subsequently, the membranes were incubated for 2 h with HRP-conjugated secondary antibodies (Solarbio, SE134, 1:2000) at room temperature. The blots were then developed with ECL solution (Meilunbio, MA0186), and the signals were detected using a Tanon-4600SF imaging system.

Real-time PCR

Shredded corneas were incubated in 1 mL TRIzol reagent (Invitrogen, 15596026) at room temperature for 1 min to extract total RNA, and the OD value and concentration of the extracted RNA were determined by spectrophotometer (Thermo Fisher Scientific, Nanodrop2000). The RNA was reverse transcribed into cDNA using a PrimeScript RT Reagent Kit for qPCR with gDNA Eraser (Takara, RR047A). Quantitative PCR was performed using a Real-Time PCR Detection System (Bio-Rad, CFX96) and SYBR Premix Ex Taq™ II (Takara,

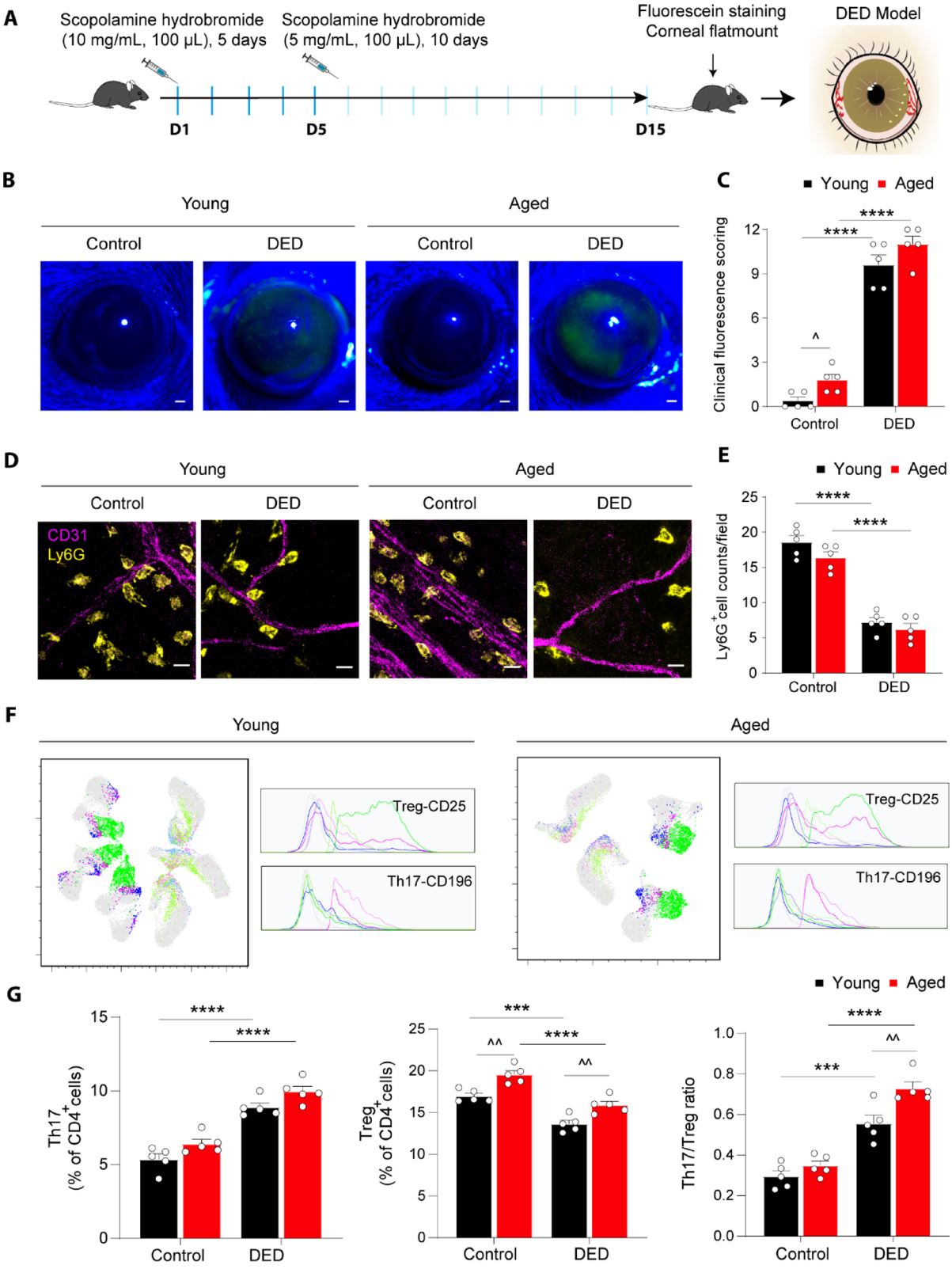

RR820A) to measure the expression of target genes. The $2^{-\Delta\Delta Ct}$ method was used to analyze gene expression relative to β-Actin, which was used as an internal control. All primers used for qPCR are listed in Supplementary Table S1.

RNA sequencing and bioinformatic analysis

Total RNA was isolated from corneal tissues, and the quality was assessed using a Nano-Photometer spectrophotometer (IMPLEN, CA, USA). Only RNA samples with an OD260/280 over 2.0 and an OD260/230 ranging from 1.8 to 2.0 were qualified for further assessment. Next, the concentration and integrity of each RNA

◀**Fig. 1**. Dry eye disease (DED) dysregulated neutrophils and Th17/Treg imbalance in the corneal limbus of a murine model. (**A**) Schematic diagram showing dry eye disease (DED) mouse model establishment. (Created with bioRender.com). (**B**) Representative fluorescein-stained images of corneas from healthy control mice (Control) and mice after 15 days of desiccating stress (DED). Scale bars, 1 mm. (**C**) Clinical fluorescence scores for corneal epithelial defects ($n = 5$). (**D**) Representative immunohistochemistry images of the corneal limbus. CD31 (magenta) indicates blood vessels, and Ly6G (yellow) indicates neutrophils. Scale bars, 10 μm. (**E**) Quantification of $Ly6G^+$ neutrophils in flat-mounted corneas, focusing on the limbus region ($n = 5$). The total number of corneal neutrophils was counted in nine 40 × fields of view that comprised the diameter of the cornea. (**F**) The proportions of Th17 ($CD4^+CD196^+$) and Treg ($CD4^+CD25^+$) cells in eye-draining lymph nodes were analyzed by flow cytometry. t-SNE plots were generated from 2×10^4 cells from the Control and DED groups ($n = 3$), with data downsampling and concatenation for inter-subject comparison. (**G**) Frequencies of Th17 cells and Treg cells and the Th17/Treg ratio in the eye-draining lymph nodes ($n = 5$). Data are presented as mean ± SEM for each group ($n = 5$). Statistical significance is denoted as $^{***}P < 0.001$, $^{****}P < 0.0001$ for DED versus Control groups and $^{\wedge}P < 0.05$, $^{\wedge\wedge}P < 0.01$ for Aged versus Young groups; *P* values were calculated using Student's *t*-test.

sample were measured using a Qubit® 2.0 Fluorometer (Life Technologies, CA, USA) and an Agilent Bioanalyzer 2100 system (Agilent Technologies, CA, USA), respectively. RNA libraries were prepared using an NEBNext® Ultra™ RNA Library Prep Kit. A Qubit2.0 Fluorometer and an Agilent Bioanalyzer 2100 were used to assess RNA concentration and integrity. Next, the libraries were sequenced on an Illumina platform, and 150-bp paired reads were generated. HISAT2 v2.0.5 was used to count the read numbers mapped to each gene. Data visualization were performed using R Studio v4.2.2 (https://posit.co/download/rstudio-desktop) Differential gene expression analysis was performed using the DESeq2 method. Genes with *P* values < 0.01 and $|\log_2(FC)| \geq 1.5$ were defined as differentially expressed genes (DEG). Gene Ontology (GO) analysis of the differentially expressed genes were performed using GOseq R. Bar charts and volcano plots were generated from the bioinformatics results using ggplot2 v3.3.2.

Magnetic cell sorting of neutrophils

Neutrophils collected from lymph nodes were isolated using magnetic beads according to the manufacturer's protocol. Eye-draining lymph node tissues were homogenized, and the cell suspension was passed through a 30-μm filter to generate a single-cell suspension. The volume of the filtrate was adjusted to 500 μL for subsequent magnetic bead sorting. A total of 5×10^7 cells was resuspended in 200 μL cell staining buffer, 50 μL of neutrophil biotin-antibody cocktail was added, and the mixture was incubated for 10 min at 4 °C. Then, 100 μL of anti-biotin microbeads was added, and the mixture was incubated for 15 min at 4 °C. Next, the mixture was added to a separation column and placed on a MACS separator, and the beads were washed with buffer (MS Separation Column: 3 × 500 μL; LS Separation Column: 3 × 3 mL). Finally, elution buffer was added to the column, and the eluate containing unlabeled neutrophils was collected.

Graphical visualization

All scientific illustrations and schematics were created using BioRender.com (https://www.biorender.com/). Proper licensing and permissions were obtained for all graphical elements used in the figures. Final image adjustments and layouts were processed using Adobe Illustrator 2020 (https://www.adobe.com/products/illustrator.html).

Statistical analysis

All data are expressed as mean ± standard error of the mean (SEM). Data were analyzed and visualized using GraphPad Prism v10.2.3 (https://www.graphpad.com/). Statistical differences between groups were analyzed by one-way ANOVA and Student's *t* test. Values of $P < 0.05$ were defined as significant statistically.

Results

Dry eye symptoms trigger aberrant neutrophil response and Th17/Treg cells imbalance in DED mice

Given that there are multiple causes of DED, including both corneal epithelial damage and inflammatory factors, we first asked whether UCMSC-Exos repaired corneal damage in vivo. To test this, we established a mouse model of DED as previously described[34] and assessed corneal defects, neutrophil counts, and the Th17/Treg ratio on day 15. Corneal fluorescein staining scores were significantly higher on day 15 than at baseline in both young and aged mice. DED induced markedly more severe epithelial defects in aged mice than in young mice (Fig. 1B and C). Given that neutrophils are the first responder of the innate immune response and are abundant in the ocular surface of patients with DED[35], we quantified neutrophils in the cornea limbus in our DED model and found that DED induced a marked decrease in neutrophil counts in the corneal limbus (Fig. 1D and E). Th17/Treg imbalance is a critical biological event during DED pathogenesis[36]; therefore, we analyzed eye-draining lymph nodes cells by flow cytometry. We noted increased frequencies of CD196-expressing $CD4^+$ T lymphocytes (Th17 cells) as well as decreased frequencies of CD25-expressing $CD4^+$ T lymphocytes (Tregs) in the DED group compared to controls (Fig. 1F and G). These results indicated that we successfully established the mouse model of DED.

UCMSC-Exos alleviate corneal surface damage and promote ocular surface repair

To evaluate the effects of UCMSC-Exos on human corneal epithelial cells, we first purified UCMSC-Exos using a previously described technique[37] (Fig. 2A). Electron microscopy demonstrated that the exosomes presented the typical ultramicroscopic structure of exosome bilayer vesicles with a dish shape (Fig. 2B). Furthermore, the peak particle size of the UCMSC-Exos was 136.3 nm, which is consistent with a typical exosome particle size between 30 and 160 nm[38] (Fig. 2C). Western blot analysis demonstrated that UCMSC-Exos expressed exosomal markers including CD9, CD63, ANXA1, CD81 and TSG101 at high levels (Fig. 2D).

Next, we investigated the effects of UCMSC-Exos on HCEC cell migration in vitro. To test this, a scratch wound was made, the cells were treated with PBS or UCMSC-Exos, and the wound area was observed 0 h, 12 h, and 24 h later. Compared with the Control group, UCMSC-Exo treatment appeared to accelerate cell migration and promote faster wound healing (Supplementary Fig. S1). These findings indicated that UCMSC-Exos may play a role in HCEC migration.

Mice with DED were treated with UCMSC-Exos (2.5×10^{10} particles/mL) either in the form of eye drops administered at a volume of 5 μL per drop, twice a day for 7 consecutive days (Exo eyedrop group), as described previously[30], or via a single tail vein injection on day 0 (Exo *i.v.* group) (Fig. 2E). Treatment with UCMSC-Exos partially restored corneal fluorescein staining scores and aqueous tear secretion in both the Exo group and the Exo *i.v.* group (Fig. 2F and G). The effects were more pronounced in young mice than in aged mice, possibly because they had milder symptoms at baseline. Notably, systemic administration through tail vein injection was more effective than UCMSC-Exo eyedrops. These findings demonstrated that UCMSC-Exos can effectively ameliorate DED symptoms.

UCMSC-Exos alter neutrophil response and the balance of Th17/Treg cells to suppress inflammation-related pathways activated by DED

To investigate the underlying mechanisms by which UCMSC-Exos inhibit the immune response in DED, we performed transcriptome sequencing of corneal tissues collected from control mice, DED mice, and DED mice treated with UCMSC-Exos by tail vein injection or via eyedrops. Differential mRNA profile analysis revealed that 488 genes were significantly upregulated and 335 genes were downregulated in the DED group compared to the control group (Fig. 3A). GO dataset analysis identified significant alterations in pathways related to cell-activated immune responses (biological processes), including the immune response-activating signaling pathway, innate immune response-activating signaling pathway, cytokine-mediated signaling pathway, T cell migration, wound healing, regulation of inflammatory response, and leukocyte migration (Fig. 3B). A heatmap further confirmed that pathways associated with lymphocyte activation were upregulated in the DED group (Fig. 3C). Importantly, these pathways were downregulated by UCMSC-Exo treatment (Fig. 3C).

Given that a previous study showed an imbalance in Th17 and Treg cell infiltration into the corneal and conjunctival tissues of patients with DED[39], we next asked whether UCMSC-Exos could decrease immune dysregulation in our murine model of DED. First, neutrophils in the corneal limbus were quantified in healthy mice, DED mice, and DED mice treated with UCMSC-Exos by manually counting $Ly6G^+$ neutrophils. Treatment with UCMSC-Exos by either tail vein injection or eyedrops rescued the abnormally decrease in neutrophil counts seen in the corneal limbus of DED mice (Fig. 4A and B). Furthermore, flow cytometry also demonstrated UCMSC-Exo enhanced proliferative capacity of corneal epithelial cells in DED mice (Supplementary Fig. 2A and B). In addition, UCMSC-Exo treatment alleviated DED-induced neutrophil recruitment (Supplementary Fig. 2C) and restored the numbers of Th17 and Treg cells, as well as the Th17/Treg ratio, to normal levels (Fig. 4C and D). Notably, the number of neutrophils in the cornea was negatively correlated with the Th17/Treg ratio in the eye-draining lymph nodes (Supplementary Fig. 2D). Consistent with our earlier results, younger mice exhibited better responses to UCMSC-Exo treatment than aged mice, and systemic administration through tail vein injection was more effective than UCMSC-Exo eyedrops.

Taken together, these results suggested the neutrophils may mediate the beneficial effects of UCMSC-Exos on DED, potentially through modulating the Th17/Treg cells balance in the eye-draining lymph nodes.

UCMSC-Exos modulate the cytokine profiles of neutrophils in eye-draining lymph nodes and corneal tissues of DED mice

Given the key role that neutrophils play in DED pathogenesis, next we sought to identify specific factors that induce neutrophil dysfunction in DED. To do this, we isolated neutrophils from mouse eye-draining lymph nodes and analyzed their expression of pro- and anti-inflammatory cytokines by qPCR. We observed an increase in the mRNA levels of the proinflammatory cytokines *Il-1β* and *Il-17* and a decrease in the levels of the anti-inflammatory factors *Arg-1*, *Il-10*, and *Tgf-β* (Fig. 5A and E). Intravenous administration of UCMSC-Exos was more effective than UCMSC-Exo eyedrops, and the young mice showed greater sensitivity to UCMSC-Exo treatment than the aged mice (Fig. 5A and E).

We further investigated the expression of immune factors in the cornea during DED by performing qPCR analysis of corneal tissue. The corneas of DED mice exhibited upregulation of proinflammatory cytokine-related genes, including *Il-1β*, *Ifn-γ*, *Il-17* and *Tnf-α*, as well as downregulation of anti-inflammatory cytokine-related genes, including *Il-10*, *Arg-1*, and *Tgf-β* (Fig. 5F and L). UCMSC-Exo treatment restored the expression levels of these cytokines in the cornea to near-normal levels.

Taken together, these findings indicated the contribution of UCMSC-Exo treatment on modulating abnormal pro- and anti-inflammatory cytokine expression by neutrophils, which could help restore Treg/Th17 cell balance in DED.

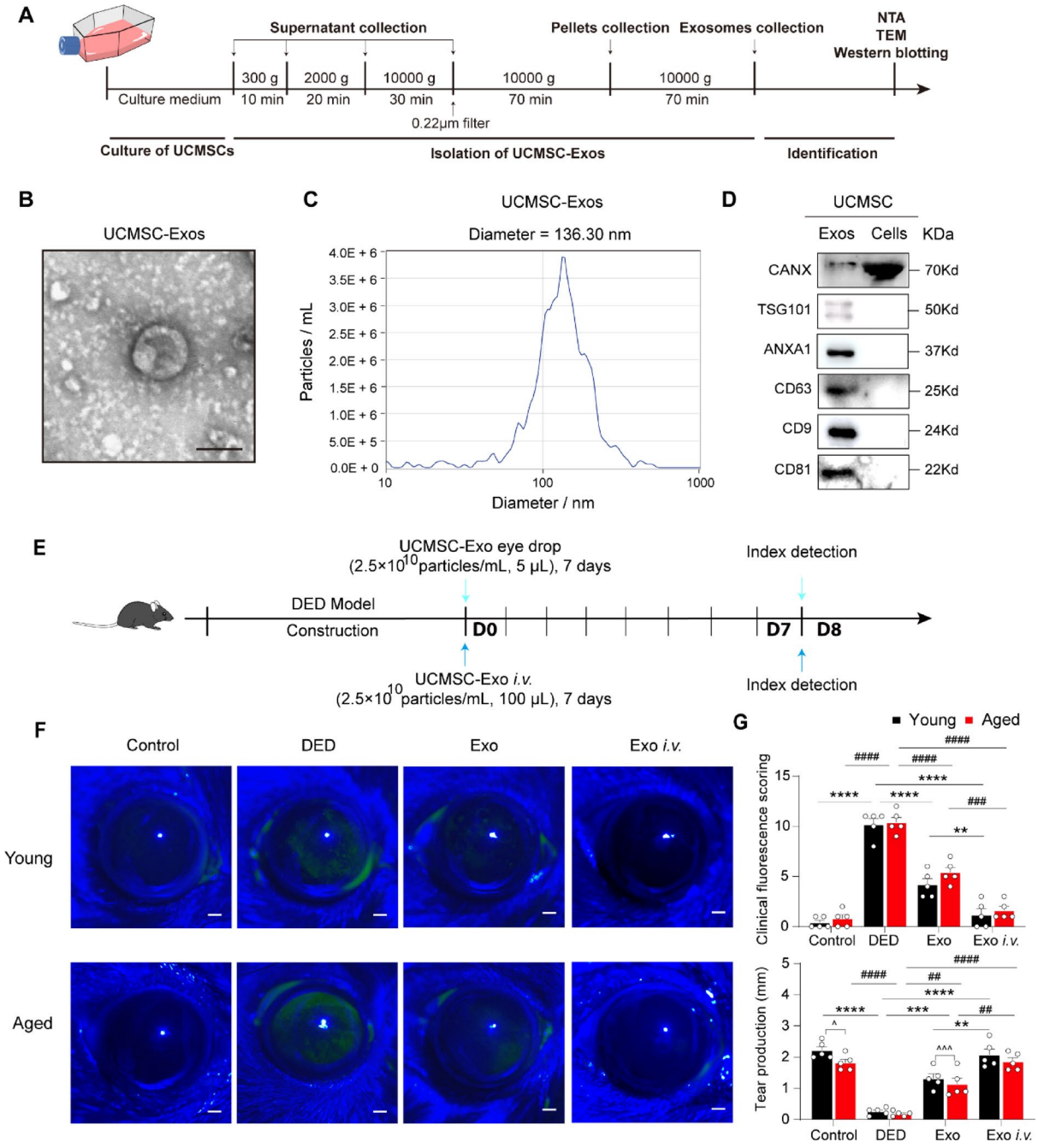

Fig. 2. Umbilical cord mesenchymal stem cell-derived exosomes (UCMSC-Exos) mitigate corneal epithelial cell damage in vivo. (**A**) Schematic diagram illustrating the UCMSC-Exo isolation procedure. (Created with bioRender.com). (**B**) Representative transmission electron microscopy (TEM) images showing the ultrastructure of the isolated UCMSC-Exos. Scale bars, 100 nm. (**C**) Size distribution of UCMSC-Exos as determined by nanoparticle tracking analysis. (**D**) Western blot analysis of TSG101, ANXA1, CD9, CD63, CD81, and ER marker CANX expression in UCMSC-Exos and UCMSCs. (**E**) Schematic diagram illustrating the UCMSC-Exo application procedure. (Created with bioRender.com). (**F**) Representative images of corneal fluorescein staining showing epithelial damage. Scale bars, 1 mm. (**G**) Clinical scores for corneal epithelial defects and tear production, as measured by Schirmer's strip test. Data are presented as mean ± SEM for each group ($n = 5$). Statistical significance is denoted as $^{**}P < 0.01$, $^{***}P < 0.001$, $^{****}P < 0.0001$ for the Young group; $^{\#\#}P < 0.01$, $^{\#\#\#}P < 0.001$, $^{\#\#\#\#}P < 0.0001$ for the Aged group; and $^{\wedge}P < 0.05$, $^{\wedge\wedge\wedge}P < 0.001$ for comparisons between the Young and Aged groups. Statistical analyses were performed by one-way ANOVA and Student's *t*-test.

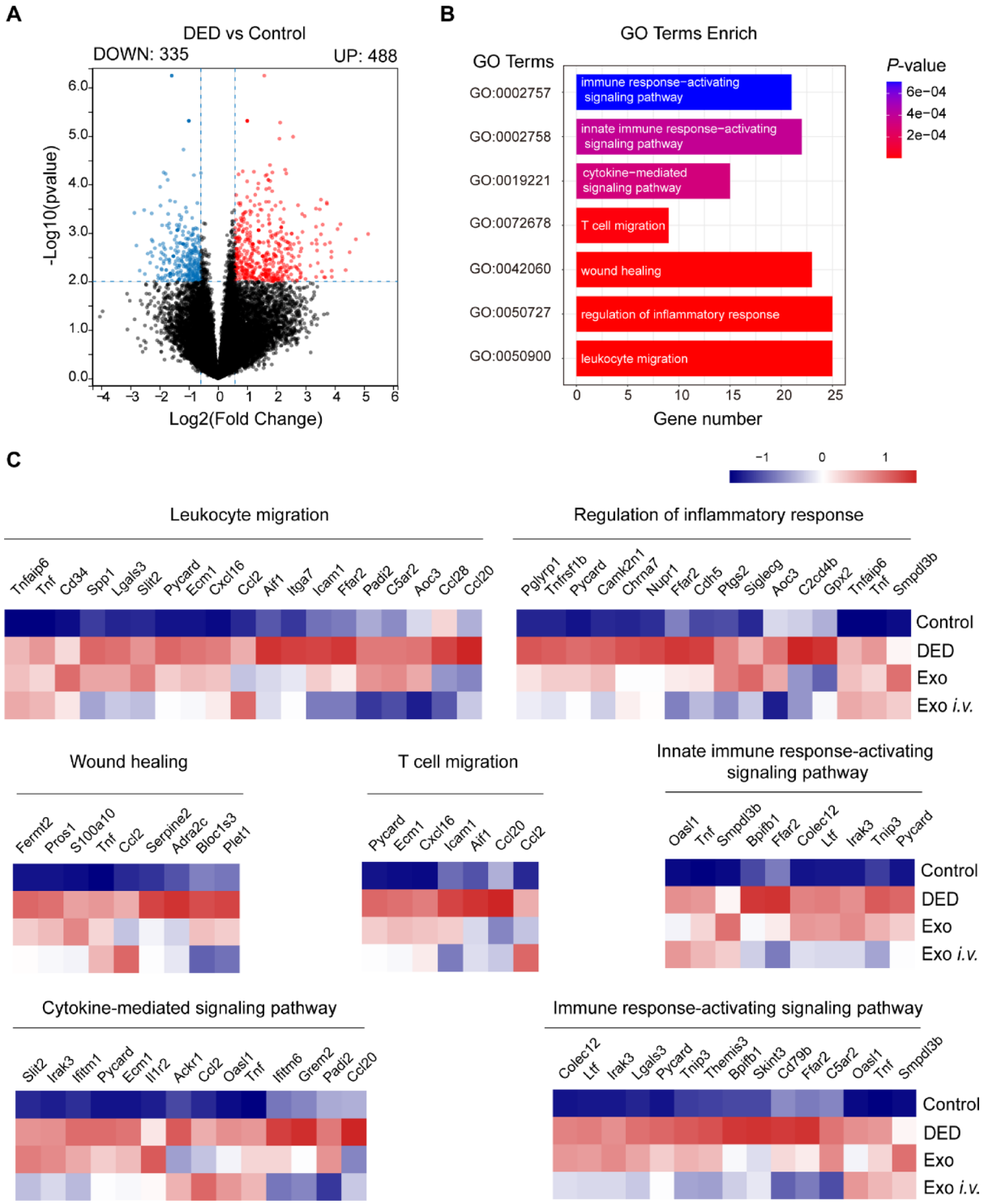

Fig. 3. Transcriptomic analysis of corneal tissue from a mouse model of DED treated with UCMSC-Exos or left untreated. (**A**) Volcano plot showing differentially expressed genes (DEGs) in the DED group compared to the control group. (**B**) GO enrichment analysis of the DEGs (488 upregulated and 335 downregulated genes), highlighting pathways that were enriched in the DED group vs. the Control group. (**C**) Heatmap displaying hierarchical clustering of the gene expression profiles of the Control, DED, Exo, and Exo *i.v.* groups. Red indicates upregulated genes, and blue indicates downregulated genes. Each group contains three independent samples.

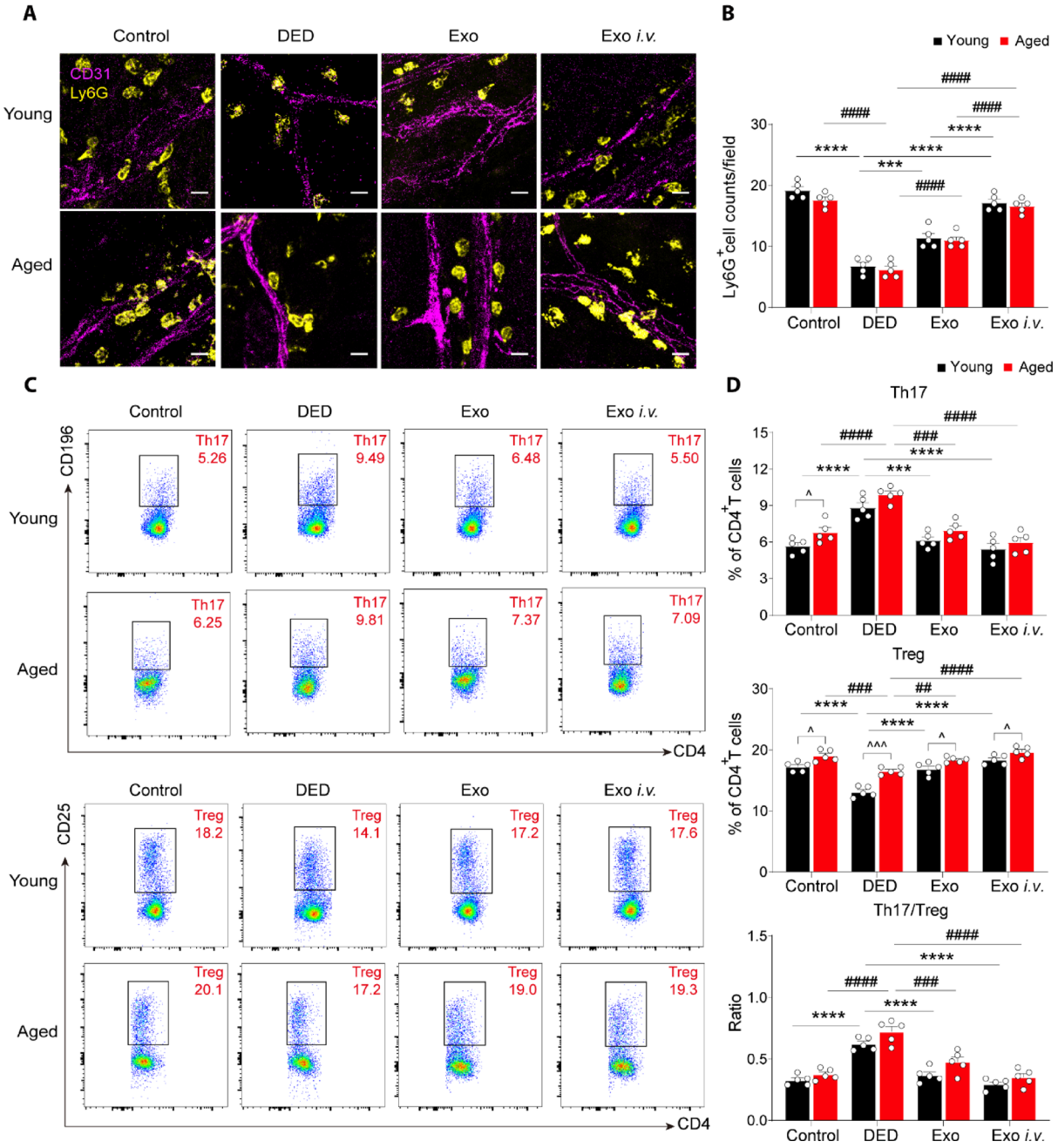

Fig. 4. UCMSC-Exos decreased neutrophil counts in the corneal limbus. (**A**) Representative immunohistochemistry images of the corneal limbus region. CD31 (magenta) indicates blood vessels, and Ly6G (yellow) indicates neutrophils. Scale bars, 10 μm. (**B**) Quantification of $Ly6g^+$ neutrophils was performed on flat-mounted corneas, focusing on the limbus region ($n = 5$). The total number of corneal neutrophils was counted in nine 40 × fields of view that comprised the diameter of the cornea. (**C**) Representative flow cytometry plots showing the frequencies of Th17 cells ($CD4^+CD196^+$) and Treg cells ($CD4^+CD25^+$) in eye-draining lymph nodes. (**D**) Quantification of Th17 cells and Treg cells and the Th17/Treg ratio ($n = 5$). Data are presented as mean ± SEM for each group ($n = 5$). Statistical significance is denoted as $^{***}P < 0.001$, $^{****}P < 0.0001$ for the Young group; $^{\#\#}P < 0.01$, $^{\#\#\#}P < 0.001$, $^{\#\#\#\#}P < 0.0001$ for the Aged group; and $^{\wedge}P < 0.05$, $^{\wedge\wedge\wedge}P < 0.001$ for comparisons between the Young and Aged groups. Statistical analyses were performed by one-way ANOVA and Student's *t*-test.

Discussion

DED is a prevalent, multifactorial inflammatory disorder of the lacrimal functional unit, resulting in chronic ocular surface damage, visual impairment, and various complications that ultimately diminish quality of life[40]. Over the past decade, exosomes derived from MSCs have emerged as key mediators of immune regulation and have been reported as potential therapeutic approaches for DED[41]. In our study, we demonstrate the effects of

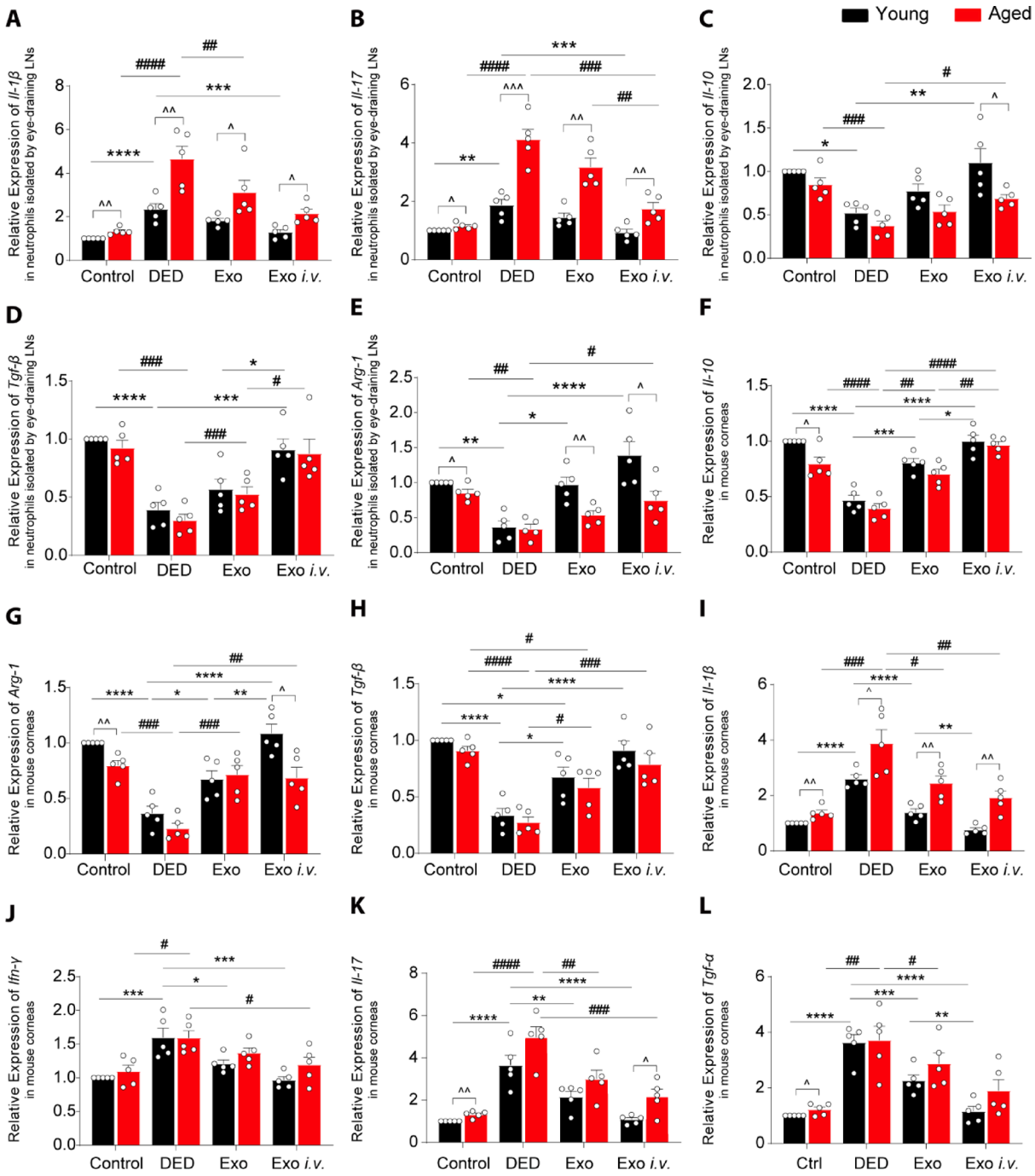

Fig. 5. UCMSC-Exos reduced inflammatory cytokine expression in neutrophils isolated from eye-draining lymph nodes and in corneal tissues. qPCR analysis *Il-1β* (**A**), *Il-17* (**B**), *Il-10* (**C**), *Tgf-β* (**D**), and *Arg-1* (**E**) expression by neutrophils isolated from eye-draining lymph nodes. qPCR analysis of *Il-10* (**F**), *Arg-1* (**G**), *Tgf-β* (**H**), *Il-1β* (**I**), *Ifn-γ* (**J**), *Il-17* (**K**) and *Tnf-α* (**L**) expression in mouse corneas. Data are presented as mean ± SEM for each group ($n = 5$). Statistical significance is denoted as follows: $^{*}P < 0.05$, $^{**}P < 0.01$, $^{***}P < 0.001$, $^{****}P < 0.0001$ for the Young group; $^{\#}P < 0.05$, $^{\#\#}P < 0.01$, $^{\#\#\#}P < 0.001$, $^{\#\#\#\#}P < 0.0001$ for the Aged group; and $^{\wedge}P < 0.05$, $^{\wedge\wedge}P < 0.01$, $^{\wedge\wedge\wedge}P < 0.001$ for comparisons between the Young and Aged groups. Statistical analyses were performed by one-way ANOVA and Student's *t*-test.

UCMSC-Exos treatment on alleviation of DED symptoms in a murine model[34]. We first established a DED model as previously reported and administered UCMSC-Exos via eyedrops and intravenous injection. We observed significant remission of corneal epithelial damage, and simultaneously repaired tear secretion. Further investigations were performed and discovered that in this model, UCMSC-Exos recruited neutrophil infiltration at the corneal limbus region. Meanwhile, the treatment of UCMSC-Exos reduced pro-inflammatory cytokines, and increased anti-inflammatory mediators significantly as well. It is worth noting that, in ocular-draining

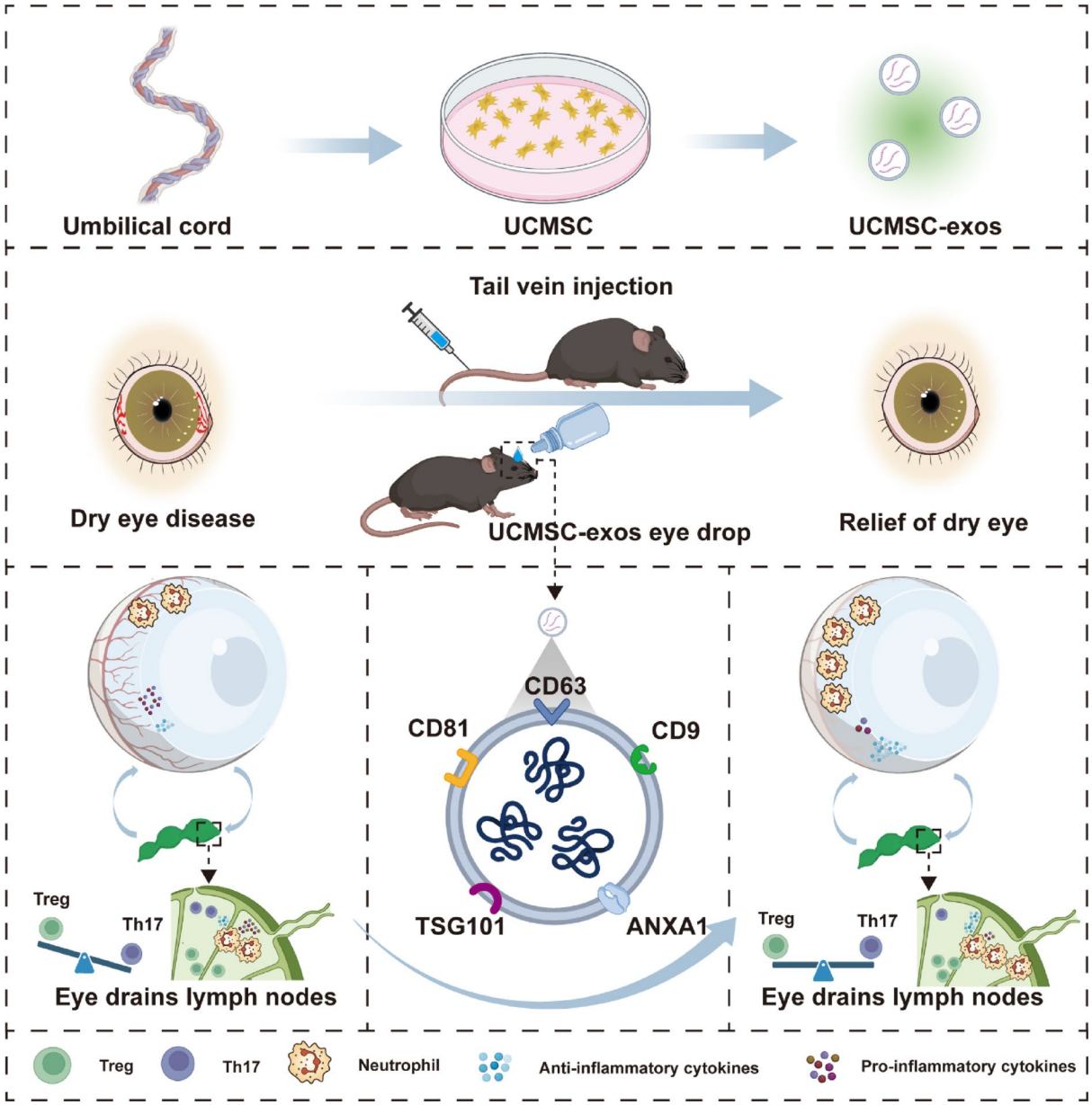

Fig. 6. Schematic drawing showing that UCMSC-Exos alleviate DED pathogenesis by modulating neutrophils on Th17/Treg balance. UCMSC-Exo treatment decreases pro-inflammatory cytokine expression and increases anti-inflammatory cytokine expression in neutrophils isolated by eye draining lymph nodes and in corneas, thereby promoting recovery of Treg/Th17 cell balance, which reduced corneal epithelial damage in dry eye. (Created with bioRender.com).

lymph nodes which serve as critical secondary lymphoid organs for antigen presentation and immune cell priming in ocular surface diseases, UCMSC-Exos treatment significantly decreased pro-inflammatory cytokines and increased anti-inflammatory cytokines, ultimately normalized the cell ratio and restored Th17/Treg cells balance (Fig. 6), which is the indicative of an improved ocular immune microenvironment. We also performed in vitro scratch assays using HCECs and confirmed the direct effects of UCMSC-Exos on promoting HCECs migration. In this study, we also discovered that the therapeutic effects of UCMSC-Exos were more pronounced in young mice as compared with aged mice. And systemic administration exhibited superior efficacy over topical application. Taken together, our findings highlighted that UCMSC-Exos served as a significant therapeutic strategy for DED treatment by regulating the immune microenvironment in mice. This approach may provide a more effective option for achieving improved clinical outcomes in DED patients.

Previous study suggested the effects of topical treatment with exosomes derived from MSCs on corneal scarring in a rat model accompanied with reduced levels of the pro-inflammatory cytokines IL-1β, IL-8, and TNF-α, and increased anti-inflammatory cytokine IL-10 production[42]. Consistently, we found that UCMSC-Exos modulate cytokine expression in neutrophils isolated by eye-draining lymph nodes and corneal tissues,

respectively. By regulating key inflammatory mediators such as TNF-α, and IFN-γ, UCMSC-Exos ameliorated the inflammatory microenvironment in DED. Recent studies have shown that MSC-Exos contain a variety of bioactive proteins (growth factors, immunomodulatory molecules, cytokines, and chemokines) as well as lipids and microRNAs (miRNAs), which can affect the survival, proliferation, phenotype and function of immune cells in the eye[43]. Previsou investigations demonstrated that MSC-Exos alleviate DED symptoms through miR-21-5p-mediated NF-kappaB pathway or aquaporin 5-mediated PKA/CREB pathway, suggesting MSC-Exos as a promising therapeutic avenue[44,45]. Further research is needed to determine the specific substances by which UMSC-Exos regulate cytokine expression in the DED model. Moreover, administering eyedrops containing exosomes from adipose-derived MSCs to a mouse model of dry eye decreased IL-1β, IL-1α, IFN-γ, and TNF-α expression and increased IL-10 expression[46]. Consistently, in our study, we found that UCMSC-Exos modulate cytokine expression in neutrophils isolated by eye-draining lymph nodes and corneal tissues, respectively. UCMSC-Exos mitigated the inflammatory microenvironment induced by DED, characterized as decreased inflammatory mediators such as TNF-α, and IFN-γ. Thus, exosomes from a variety of stem cells, including UCMSCs, may be an effective therapeutic approach to addressing the immune-driven components of DED, offering a dual benefit of repairing ocular surface damage and resolving chronic inflammation.

Although numerous studies have explored immune responses in DED-associated corneal epitheliopathy—including natural killer cell activation, Toll-like receptor signaling, pro-inflammatory cytokine/chemokine secretion, corneal antigen-presenting cell maturation, and T-cell-mediated inflammatory responses[47,48]—our study revealed a previously underappreciated dysregulation of neutrophil in dry eye mice, highlighting the involvement of innate immunity in DED pathogenesis. In our study, we found that DED induced a decrease in neutrophil infiltration at the corneal limbus. This is consistent with a previous study that showed a decrease in lymph node polymorphonuclear neutrophil counts in female mice subjected to desiccating stress[34]. We then focused on the changes of neutrophils during DED process and after UCMSC-Exo treatment to explore the specific mechanisms of DED development. To be noted, the increase in neutrophils in response to UCMSC-Exo treatment observed in our study negatively correlated with the Th17/Treg ratio, suggesting a link between the innate and adaptive immune response in DED pathogenesis. Future studies should be performed to investigate the role of exosomes in mediating interactions between lymphocytes and neutrophils in the context of DED.

While both local and systemic administration of UCMSC-Exos had beneficial effects on DED in our study, intravenous injection was more effective than application via eyedrops, highlighting its potential as the preferred delivery route for future exosome-based treatments in DED. This is consistent with earlier studies indicating that intravenous infusion of MSCs shows remarkable therapeutic efficacy in addressing systemic inflammation[49].

Most of the studies on dry eye disease use 6 to 8-week-old mice as disease model[50]. However, elderly women, a high-risk group for dry eye disease, have received relatively less research attention[51]. A novelty of our study is that we tested the therapeutic effect of UCMSC-Exo on both young and old mice (a total of 44 mice) with dry eye disease. We found that the severity of DED in 50-week-old mice was higher than that in 15-week-old mice, and the benefit of UCMSC-Exo treatment for young mice was greater than that for elderly mice. These results underscore the importance of developing age-specific treatment strategies, particularly for elderly female patients who represent a high-risk demographic for DED but remain understudied in preclinical research.

Our study had several limitations. DED often involves long-term adaptive immune responses and tissue remodeling. It should be noticed that the conventional endpoint (15-day) which we chose to establish the DED mouse model does not fully replicate the complex and chronic nature of human DED. Future studies should be conducted to evaluate in chronic DED models at 1, 3, and 6 months post-treatment to determine whether UCMSC-Exos provides sustained relief or requires repeated administration for lasting benefits. Additionally, the key microRNAs and relative regulatory pathways underlying the therapeutic effect of UCMSC-Exos on the neutrophil-Th17/Treg axis remain unclear. Future studies should perform multi-omics analysis and functional validation experiments to identify key microRNAs and signaling pathways.

In conclusion, our study revealed the multifaceted immunomodulatory function of UCMSC-Exos, which laid a crucial foundation for further in-depth investigations. More important, this research provided profound insights into the remarkable therapeutic potential of UCMSC-Exos, while establishing a theoretical framework for the future development of MSC-based therapies for a wide range of diseases. Both local and systemic treatment with UCMSC-Exos was discovered on their effective alleviation of DED pathogenesis through regulating the immune response and repairing epithelial cells, especially in young female mice. Our findings emphasize the role of the innate immune system in DED pathogenesis and show for the first time that UCMSC-Exos alleviate inflammation by regulating cytokine production by neutrophils. We also highlight the superiority of systemic treatment in addressing this disease. These preclinical findings position UCMSC-Exos as a transformative cell-free therapy for DED. Crucially, UCMSC-Exos circumvent challenges associated with live-cell therapies, including tumorigenic risks and ethical constraints, while offering scalable production and standardized formulation—key prerequisites for clinical translation.

Data availability

The datasets generated and analysed during this study are available in the the National Center for Biotechnology Information (NCBI) Gene Expression Omnibus (GEO) repository under accession number GSE316045.

Received: 23 July 2025; Accepted: 28 January 2026
Published online: 05 February 2026

References

1. Sheppard, J., Shen Lee, B. & Periman, L. M. Dry eye disease: Identification and therapeutic strategies for primary care clinicians and clinical specialists. *Ann. Med.* **55**, 241–252. https://doi.org/10.1080/07853890.2022.2157477 (2023).
2. Stapleton, F. et al. TFOS DEWS II epidemiology report. *Ocul Surf.* **15**, 334–365. https://doi.org/10.1016/j.jtos.2017.05.003 (2017).
3. Hakim, F. E. & Farooq, A. V. Dry eye disease: An update in 2022. *JAMA* **327**, 478–479. https://doi.org/10.1001/jama.2021.19963 (2022).
4. Auffret, E. et al. Digital eye strain. Symptoms, prevalence, pathophysiology, and management. *J. Fr. Ophtalmol.* **44**, 1605–1610. https://doi.org/10.1016/j.jfo.2020.10.002 (2021).
5. Zoukhri, D. Effect of inflammation on lacrimal gland function. *Exp. Eye Res.* **82**, 885–898. https://doi.org/10.1016/j.exer.2005.10.018 (2006).
6. Periman, L. M., Perez, V. L., Saban, D. R., Lin, M. C. & Neri, P. The immunological basis of dry eye disease and current topical treatment options. *J. Ocul Pharmacol. Ther.* **36**, 137–146. https://doi.org/10.1089/jop.2019.0060 (2020).
7. Lio, C. T., Dhanda, S. K. & Bose, T. Cluster analysis of dry eye disease models based on immune cell parameters—new insight into therapeutic perspective. *Front. Immunol.* **11**, 1930. https://doi.org/10.3389/fimmu.2020.01930 (2020).
8. Levine, H. et al. Relationships between activated dendritic cells and dry eye symptoms and signs. *Ocul Surf.* **21**, 186–192. https://doi.org/10.1016/j.jtos.2021.06.001 (2021).
9. Aggarwal, S. et al. Correlation of corneal immune cell changes with clinical severity in dry eye disease: An in vivo confocal microscopy study. *Ocul Surf.* **19**, 183–189. https://doi.org/10.1016/j.jtos.2020.05.012 (2021).
10. Nair, A. P. et al. Altered ocular surface immune cell profile in patients with dry eye disease. *Ocul Surf.* **21**, 96–106. https://doi.org/10.1016/j.jtos.2021.04.002 (2021).
11. Chen, Y. et al. IFN-gamma-expressing Th17 cells are required for development of severe ocular surface autoimmunity. *J. Immunol.* **199**, 1163–1169. https://doi.org/10.4049/jimmunol.1602144 (2017).
12. Ratay, M. L. et al. Treg-recruiting microspheres prevent inflammation in a murine model of dry eye disease. *J. Control Release.* **258**, 208–217. https://doi.org/10.1016/j.jconrel.2017.05.007 (2017).
13. Hu, J. et al. Erxian decoction modulates Th17/Treg cells differentiation through LFA-1/ICAM-1/STAT3 pathway in menopausal dry eye disease. *Exp. Eye Res.* **215**, 108890. https://doi.org/10.1016/j.exer.2021.108890 (2022).
14. Roda, M. et al. Dry eye disease and tear cytokine Levels—a meta-analysis. *Int. J. Mol. Sci.* https://doi.org/10.3390/ijms21093111 (2020).
15. Kumar, N. R. et al. Tear biomarkers in dry eye disease: Progress in the last decade. *Indian J. Ophthalmol.* **71**, 1190–1202. https://doi.org/10.4103/IJO.IJO_2981_22 (2023).
16. Ogawa, Y., Takeuchi, T. & Tsubota, K. Autoimmune epithelitis and chronic inflammation in Sjogren's syndrome-related dry eye disease. *Int. J. Mol. Sci.* https://doi.org/10.3390/ijms222111820 (2021).
17. Carreno-Galeano, J. T., Dohlman, T. H., Kim, S., Yin, J. & Dana, R. A. Review of ocular Graft-versus-Host disease: Pathophysiology, clinical presentation and management. *Ocul Immunol. Inflamm.* **29**, 1190–1199. https://doi.org/10.1080/09273948.2021.1939390 (2021).
18. Kowalski, M. L. et al. Classification and practical approach to the diagnosis and management of hypersensitivity to nonsteroidal anti-inflammatory drugs. *Allergy* **68**, 1219–1232. https://doi.org/10.1111/all.12260 (2013).
19. Bain, C. R., Myles, P. S., Corcoran, T. & Dieleman, J. M. Postoperative systemic inflammatory dysregulation and corticosteroids: A narrative review. *Anaesthesia* **78**, 356–370. https://doi.org/10.1111/anae.15896 (2023).
20. Ramos-Casals, M. et al. EULAR recommendations for the management of Sjogren's syndrome with topical and systemic therapies. *Ann. Rheum. Dis.* **79**, 3–18. https://doi.org/10.1136/annrheumdis-2019-216114 (2020).
21. McInnes, I. B. & Gravallese, E. M. Immune-mediated inflammatory disease therapeutics: Past, present and future. *Nat. Rev. Immunol.* **21**, 680–686. https://doi.org/10.1038/s41577-021-00603-1 (2021).
22. Ceylanoglu, K. S. & Sen, E. M. The effect of topical steroids and non-steroidal anti inflammatory drugs on epiphora of unknown cause: Optical coherence tomography study. *Photodiagnosis Photodyn Ther.* **41**, 103234. https://doi.org/10.1016/j.pdpdt.2022.103234 (2023).
23. Rigas, B., Huang, W. & Honkanen, R. NSAID-induced corneal melt: Clinical importance, pathogenesis, and risk mitigation. *Surv. Ophthalmol.* **65**, 1–11. https://doi.org/10.1016/j.survophthal.2019.07.001 (2020).
24. Stern, J. H. et al. Regenerating eye tissues to preserve and restore vision. *Cell. Stem Cell.* **22**, 834–849. https://doi.org/10.1016/j.stem.2018.05.013 (2018).
25. Derks, L. L. M. & van Boxtel, R. Stem cell mutations, associated cancer risk, and consequences for regenerative medicine. *Cell. Stem Cell.* **30**, 1421–1433. https://doi.org/10.1016/j.stem.2023.09.008 (2023).
26. Lim, J. M., Lee, M., Lee, E. J., Gong, S. P. & Lee, S. T. Stem cell engineering: Limitation, alternatives, and insight. *Ann. N Y Acad. Sci.* **1229**, 89–98. https://doi.org/10.1111/j.1749-6632.2011.06093.x (2011).
27. Kalluri, R. & LeBleu, V. S. The biology, function, and biomedical applications of exosomes. *Science* https://doi.org/10.1126/science.aau6977 (2020).
28. Pegtel, D. M., Gould, S. J. Exosomes *Annu. Rev. Biochem.* **88**, 487–514. https://doi.org/10.1146/annurev-biochem-013118-111902 (2019).
29. Jiang, Y., Lin, S. & Gao, Y. Mesenchymal stromal cell-based therapy for dry eye: Current status and future perspectives. *Cell. Transpl.* **31**, 9636897221133818. https://doi.org/10.1177/09636897221133818 (2022).
30. Zhou, T. et al. miR-204-containing exosomes ameliorate GVHD-associated dry eye disease. *Sci. Adv.* **8**, eabj9617. https://doi.org/10.1126/sciadv.abj9617 (2022).
31. Wang, Y. et al. Umbilical cord mesenchymal stem cell-derived apoptotic extracellular vesicles ameliorate cutaneous wound healing in type 2 diabetic mice via macrophage pyroptosis inhibition. *Stem Cell. Res. Ther.* **14**, 257. https://doi.org/10.1186/s13287-023-03490-6 (2023).
32. Yoon, K. C. et al. Tear production and ocular surface changes in experimental dry eye after elimination of desiccating stress. *Invest. Ophthalmol. Vis. Sci.* **52**, 7267–7273. https://doi.org/10.1167/iovs.11-7231 (2011).
33. Chen, Y., Chauhan, S. K., Lee, H. S., Saban, D. R. & Dana, R. Chronic dry eye disease is principally mediated by effector memory Th17 cells. *Mucosal Immunol.* **7**, 38–45. https://doi.org/10.1038/mi.2013.20 (2014).
34. Gao, Y. et al. Female-specific downregulation of tissue polymorphonuclear neutrophils drives impaired regulatory T cell and amplified effector T cell responses in autoimmune dry eye disease. *J. Immunol.* **195**, 3086–3099. https://doi.org/10.4049/jimmunol.1500610 (2015).
35. Sonawane, S. et al. Ocular surface extracellular DNA and nuclease activity imbalance: A new paradigm for inflammation in dry eye disease. *Invest. Ophthalmol. Vis. Sci.* **53**, 8253–8263. https://doi.org/10.1167/iovs.12-10430 (2012).
36. Chauhan, S. K. et al. Autoimmunity in dry eye is due to resistance of Th17 to Treg suppression. *J. Immunol.* **182**, 1247–1252. https://doi.org/10.4049/jimmunol.182.3.1247 (2009).
37. Zhang, Z. et al. Comprehensive characterization of human brain-derived extracellular vesicles using multiple isolation methods: Implications for diagnostic and therapeutic applications. *J. Extracell. Vesicles.* **12**, e12358. https://doi.org/10.1002/jev2.12358 (2023).
38. Lotvall, J. et al. Minimal experimental requirements for definition of extracellular vesicles and their functions: A position statement from the international society for extracellular vesicles. *J. Extracell. Vesicles.* **3**, 26913. https://doi.org/10.3402/jev.v3.26913 (2014).
39. Barabino, S. & Dana, M. R. Dry eye syndromes. *Chem. Immunol. Allergy.* **92**, 176–184. https://doi.org/10.1159/000099268 (2007).

40. Zemanova, M. Dry eye Disease. A review. *Cesk. Slov. Oftalmol.* **77**, 107–119. https://doi.org/10.31348/2020/29 (2021).
41. Li, S. J. et al. Advances in mesenchymal stem cell-derived extracellular vesicles therapy for Sjogren's syndrome-related dry eye disease. *Exp. Eye Res.* **237**, 109716. https://doi.org/10.1016/j.exer.2023.109716 (2023).
42. Ong, H. S. et al. Mesenchymal stem cell exosomes as Immunomodulatory therapy for corneal scarring. *Int. J. Mol. Sci.* https://doi.org/10.3390/ijms24087456 (2023).
43. Randall Harrell, C., Djonov, V., Volarevic, A., Arsenijevic, A. & Volarevic, V. Mesenchymal stem Cell-Sourced exosomes as potentially novel remedies for severe dry eye disease. *J. Ophthalmol.* **2025**, 5552374. https://doi.org/10.1155/joph/5552374 (2025).
44. Zhao, D. et al. BMSC-derived exosomes regulate the Treg/Th17 balance through the miR-21-5p/TLR4/MyD88/NF-kappaB pathway to alleviate dry eye symptoms in mice. *Vitro Cell. Dev. Biol. Anim.* **60**, 644–656. https://doi.org/10.1007/s11626-024-00910-6 (2024).
45. Hu, S. et al. Dental pulp stem cell-derived exosomes revitalize salivary gland epithelial cell function in NOD mice via the GPER-mediated cAMP/PKA/CREB signaling pathway. *J. Transl. Med.* **21**, 361. https://doi.org/10.1186/s12967-023-04198-0 (2023).
46. Wang, G. et al. Exosomes derived from mouse Adipose-Derived mesenchymal stem cells alleviate Benzalkonium Chloride-Induced mouse dry eye model via inhibiting NLRP3 inflammasome. *Ophthalmic Res.* **65**, 40–51. https://doi.org/10.1159/000519458 (2022).
47. Liu, Z. et al. Single-cell landscape reveals the epithelial cell-centric pro-inflammatory immune microenvironment in dry eye development. *Mucosal Immunol.* **17**, 491–507. https://doi.org/10.1016/j.mucimm.2023.11.008 (2024).
48. Huang, D. & Li, Z. Multidimensional immunotherapy for dry eye disease: Current status and future directions. *Front. Ophthalmol. (Lausanne)*. **4**, 1449283. https://doi.org/10.3389/fopht.2024.1449283 (2024).
49. Yu, S. et al. Treatment with adipose tissue-derived mesenchymal stem cells exerts anti-diabetic effects, improves long-term complications, and attenuates inflammation in type 2 diabetic rats. *Stem Cell. Res. Ther.* **10**, 333. https://doi.org/10.1186/s13287-019-1474-8 (2019).
50. Zuo, X. et al. AKR1C1 protects corneal epithelial cells against oxidative Stress-Mediated ferroptosis in dry eye. *Invest. Ophthalmol. Vis. Sci.* **63**(10), 1–15. https://doi.org/10.1167/iovs.63.10.3 (2022).
51. Zhang, X., Wang, L., Zheng, Y., Deng, L. & Huang, X. Prevalence of dry eye disease in the elderly: A protocol of systematic review and meta-analysis. *Med. (Baltim).* **99**, e22234. https://doi.org/10.1097/MD.0000000000022234 (2020).

Acknowledgements
We thank all staff for collecting experimental data for this study.

Author contributions
YG-X Contributed to conceptualization; YG-X, YD-F, J.Y., T.D. and J.M. Conducted the experiments; YG-X, YD-F, B.L., W.S., Y.D. and Y.Z. Wrote the manuscript; YG-X, YD-F, J.Y., T.D., J.M. Contributed to methodology, validation and formal analysis; All the authors contributed to manuscript writing-original draft preparation; YG-X, YD-F, Y.D., P.D., and Y.G. Contributed to revise the manuscript. Y.G. Contributed to editing and supervision of the project; Y.G. Contributed to project administration and funding acquisition. All authors contributed to the article and approved the submitted version. All authors reviewed the manuscript.

Funding
Our work was supported by The National Key Research and Development Program of China grant 2019YFA0111200 (to Y. Gao); The National Key Research and Development Program of China grant 2020YFA0113500 (to Y. Deng); National Natural Science Foundation of China grant 82371047 (to Y. Gao); Joint Funds of the National Natural Science Foundation of China grant U23A20436 (to Y. Gao); The Key Program of Shanxi Province grant 202302130501008 (to Y. Gao); Shanxi Provincial Science Fund for Distinguished Young Scholars grant 202103021221008 (to Y. Gao); Key Innovation Teams of Shanxi Province grant 202204051001023 (to Y. Gao); Shanxi Provincial Foundation for Leaders of Disciplines in Science grant 2024Q014 (to Y. Gao); The Shanxi Provincial Foundation for Returned Scholars 2022 -117 (to Y. Gao); and Natural Science Foundation of Chongqing City grant CSTB2022NSCQ-MSX0833 (to P. Duan).

Declarations

Competing interests
The authors declare no competing interests.

Ethical approval
Human umbilical cord mesenchymal stem cells (UCMSCs) were approved by Shanxi Medical University (approval number: 2023SJL66) and conducted in accordance with the local legislation and institutional requirements. All animal experiments were approved by the Animal Care Committee of Shanxi Medical University (approval number: 2023-133) and conducted according to the institution's laboratory animal welfare guidelines.

Additional information
Supplementary Information The online version contains supplementary material available at https://doi.org/10.1038/s41598-026-38010-y.

Correspondence and requests for materials should be addressed to Y.Z. or Y.G.